Dalton Transactions

PAPER

View Article Online
View Journal | View Issue

Cite this: *Dalton Trans.*, 2014, **43**, 14798

C–H activation and metalation at electrode surfaces: 2,3-dimethyl-1,4-dihydroxybenzene on Pd(pc) and Pd(111) studied by TLE, HREELS and DFT

Alnald Javier,[a] Ding Li,[b] Juan Cruz,[b] Elizabeth Binamira-Soriaga,[b] Perla B. Balbuena[c] and Manuel P. Soriaga*[a,b]

Received 15th July 2014,
Accepted 5th August 2014

DOI: 10.1039/c4dt02137a

www.rsc.org/dalton

Previous studies, based on thin-layer electrochemistry (TLE), *in situ* scanning tunneling microscopy (EC-STM), high-resolution electron energy loss spectroscopy (HREELS) and density functional theory (DFT) computations, on the chemical adsorption of hydroquinone from aqueous solutions onto atomically smooth Pd (and Pt) electrode surfaces indicated two modes of attachment that depended upon the solution concentration. At low activities, the diphenol was oxidatively chemisorbed as benzoquinone in a flat orientation, suggestive of a Pd(2,3,5,6-η-$C_6H_4O_2$) surface complex; at higher concentrations, vertical chemisorption was effected *via* two C–H bond activations (or metalations) at the 2 and 3 ring positions, evocative of an *o*-phenylene organopalladium compound. We have extended the work to 2,3-dimethyl-1,4-dihydroxybenzene on Pd(pc) and Pd(111) electrodes to probe the effect of two methyl substituents on only one side of the diphenol ring. Surface coverage and adsorbed-molecule cross section data from TLE and HREELS measurements revealed non-random concentration-dependent adsorbate orientations similar to the oxidative chemisorption of hydroquinone: flat at low concentrations and edgewise at elevated concentrations. The DFT results suggested that, for the flat structure, surface coordination is *via* the two double bonds of the quinone ring as in [Pd(2,3,5,6-η)-2,3-dimethyl-*p*-quinone]. For the edge-vertical orientation, a structure analogous to an *o*-phenylene compound is generated in which C–H bonds at the 5 and 6 ring positions are activated and then metalated. DFT-simulated HREELS spectra helped identify the observed peaks that distinguish the surface-coordinated quinone from the surface-metalated diphenol.

Introduction

We have long held a keen interest in the use of constructs from coordination and organometallic chemistry to describe the interaction of organic compounds with transition-metal electrode surfaces.[1–5] In early work based on thin-layer electrochemistry (TLE), the chemisorption of fifty-odd aromatic and quinonoid compounds on atomically smooth (flame-annealed) polycrystalline platinum electrodes[6–10] were characterized primarily in terms of absolute surface coverages (Γ mol cm^{-2}) and adsorption isotherms [Γ *vs.* log(C°), where C° is the concentration of the adsorbate in solution]. For homocyclic compounds that had at least two adjacent C–H bonds, the isotherms invariably consisted of two constant-Γ plateaus: a lower one at $C^{\circ} \leq 0.1$ mM, and an upper plateau at $C^{\circ} \geq 1$ mM. For a better perspective, Γ may be expressed in terms of σ (Å^2 per molecule), the adsorbed-molecule cross section; $\sigma = 10^{16} (N_A\ \Gamma)^{-1}$, where N_A is Avogadro's number. A σ *vs.* log(C°) isotherm then represents the concentration-dependence of the area on the surface that is occupied by a chemisorbed molecule. Hence, σ is large when adsorption is from lower concentrations; small if from higher concentrations. Comparison of σ_{exp} with σ_{calc} for all possible aromatic configurations[11] allows the assignment of a specific orientation to a constant-σ (constant-Γ) plateau. Hence, the isotherm for 1,4-dihydroxybenzene indicated that, at $C^{\circ} \leq 0.1$ mM, the compound was oriented parallel to the surface (σ_{exp} = 52.7 Å^2 and σ_{calc} = 53.8 Å^2); at $C^{\circ} \geq 1$ mM, it was oriented edgewise at the 2,3 side (σ_{exp} = 27.9 Å^2 and σ_{calc} = 28.6 Å^2).

It was later observed, based on additional TLE evidence, such as a chemisorption-induced cathodic shift in the rest potential and a Faradaic H_2-oxidation charge, that the chemisorption process was oxidative. That is, upon adsorption in the

[a]*Joint Center for Artificial Photosynthesis, Division of Chemistry and Chemical Engineering, California Institute of Technology, Pasadena, CA 91125, USA. E-mail: msoriaga@caltech.edu*
[b]*Department of Chemistry, Texas A&M University, College Station, TX 77843, USA*
[c]*Department of Chemical Engineering, Texas A&M University, College Station, TX 77843, USA*

flat orientation, 1,4-dihydroxybenzene was oxidized to 1,4-benzoquinone accompanied by the release of H_2; it should be noted that σ_{calc} for 1,4-dihydroxybenzene is essentially the same as for 1,4-benzoquinone. Chemisorption in the edgewise orientation was likewise found to be oxidative accompanied by generation of H_2. Subsequent infrared absorption-reflection spectroscopy (IRRAS) showed hydrogen-bonded –OH stretch peaks in the vertically oriented species;[11] these results were used as evidence for the formation, not of an edge-adsorbed *p*-quinone, but of a 2,3-edge-bonded 1,4-diphenol.

The adsorption of the diphenolic and quinonoid compounds was determined to be irreversible:[1–5] copious rinses with aqueous sulfate, a weakly coordinating ligand, in the absence of applied potential did not displace the adsorbates from the surface. Electrogenerated $H_{2(g)}$, however, desorbed the original material in a reaction the reverse of oxidative chemisorption. Reductive (hydrogenative) desorption was also observed in the presence of strongly coordinating electrolytes such as iodide and sulfide that, by themselves, evolve stoichiometric amounts of $H_{2(g)}$ upon (oxidative) chemisorption. Aromatic chemisorption on Pt and Pd involves sufficiently strong organometallic chemical bonds; estimates based on a thermodynamic analysis of the chemisorption isotherms[1] indicated approximately 80 kJ mol^{-1} and 100 kJ mol^{-1} for the edge and flat orientations, respectively. Equally significant, additional kinetic stability is afforded since desorption involves hydrogenative reduction.[2]

The above studies provided the impetus for an extensive search of the rich organometallic literature for compounds that could serve as molecular models for the postulated adsorbed-aromatic orientations. Illustrative examples are shown in Fig. 1 [1]. Over the past two decades, the viability of the analogy between adsorbate orientation and molecular structure, as exemplified in Fig. 1, has been reinforced by extended studies that employed modern surface-sensitive physical and analytical techniques such as high-resolution electron-energy loss spectroscopy (HREELS),[12] *in situ* scanning tunneling microscopy,[13] Auger electron spectroscopy (AES)[14] and differential electrochemical mass spectrometry (DEMS);[15] computational work was also pursued by density functional theory.[16]

We have expanded our surface organometallic chemistry investigations to include polycrystalline (pc) and single-crystal

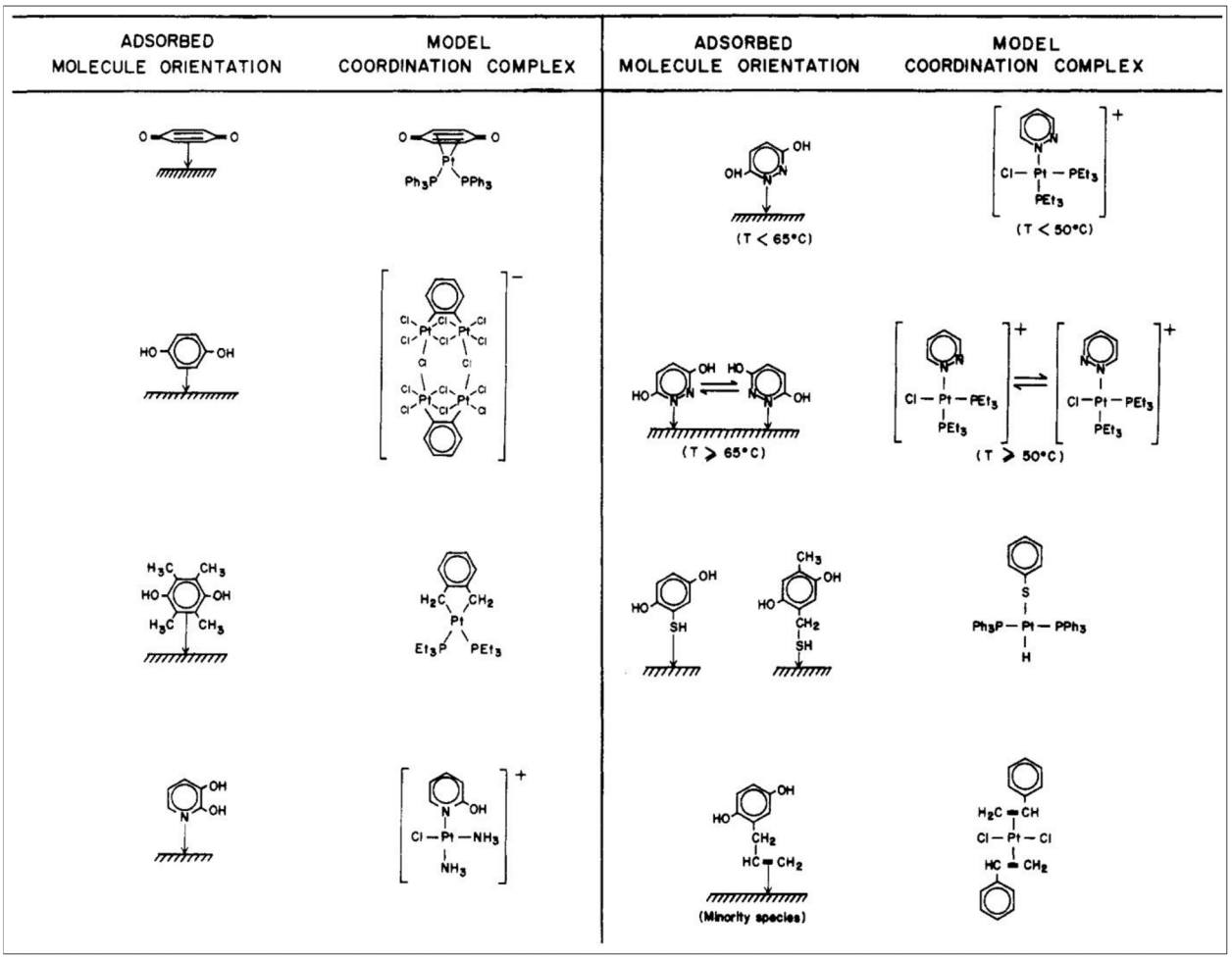

Fig. 1 Molecular coordination and organometallic compounds as models for the postulated adsorbed-molecule orientations [1]. Reprinted with permission. Copyright (1985) American Chemical Society.

(*hkl*) palladium electrode surfaces.[12,13,16] For 1,4-diphenol, we have already determined that the interfacial properties of 1,4-dihydroxybenzene on Pd and on Pt are quite similar, although the strength of aromatic–metal interactions is higher on Pt. In this manuscript, we present TLE, HREELS and DFT results for the chemisorption of 2,3-dimethyl-1,4-dihydroxybenzene (2,3-dimethyl hydroquinone) on Pd(pc) and Pd(111) electrode surfaces; the objective was to probe the effect of two methyl substituents on only one side of the diphenol ring.

Experimental

Thin-layer electrochemistry[17] is a well-documented, highly reliable and widely adopted technique in the study of the solid-electrolyte interface since the ratio of surface area (A) to solution volume (V) is nominally four orders of magnitude larger than in typical EC cells. Surface processes are thus magnified relative to those in solution; in addition, the absence of diffusional mass transport minimizes surface contamination from the bulk solution and allows the isolation of reaction products for subsequent analysis. The use of TLE to generate the empirical Γ *vs.* $\log(C^{\circ})$ isotherms, along with the algorithm to calculate σ_{calc},[18] has been detailed elsewhere[6–10,17,18] and will not be repeated here.

A commercially oriented and metallographically polished Pd(111) single crystal of 99.999% purity (MSEN Cornell University, Ithaca, NY) was used in the ultrahigh vacuum (UHV) experiments.[3,5,15] Prior to first use, it was cleaned by multiple cycles of Ar^+-ion bombardment, thermal oxidation in 10^{-6} Torr O_2, and high-temperature annealing (1020 K). Before each measurement, the crystallinity of the (111)-surface was verified by low-energy electron diffraction (LEED), and its surface cleanliness was established by AES. The highly pure polycrystalline Pd billet that was used in the TLE experiments was metallographically polished. Between experiments, the electrode was flame-annealed to maintain surface smoothness and then, to ensure surface cleanliness, subjected to oxidation-reduction cycles in 1 M H_2SO_4 between the hydrogen-evolution and oxygen-evolution regions.[6–10]

HREELS was performed in an all-stainless-steel apparatus that was also equipped with LEED and AES for surface characterization[3,5] prior to the chemisorption and HREELS experiments. An LKT spectrometer (LK Technologies, Bloomington, IN) was used with a beam energy of 4 eV, primary beam rate at 1.7×10^5 Hz (cps), and a resolution of 4.8 meV (38 cm^{-1}); spectra were collected only in the specular direction, 62° from the surface normal. Extraction of surface-coverage information from HREELS requires the normalization of integrated peak intensities to compensate for differences in the backscattered electron flux brought about by the organic adlayer. A common procedure rests on a match of the elastic-peak heights, but it fails for organic adsorbates which introduce surface roughness that result in a higher stream of inelastically scattered electrons. A more accurate method, adopted in this study, is based on the equalization of the incident electron beam currents which is attained only when the background intensities integrated over a peak-free spectral region (2100 to 2700 cm^{-1}) are set equal to one another.[19] Γ is directly proportional to the properly normalized integrated area (A_N) under a prominent and well-isolated HREELS peak.[12]

Solutions of 2,3-dimethylhydroquinone (Aldrich Chemicals, Milwaukee, WI) for the TLE measurements were prepared in 1 M H_2SO_4 with Milli-Q Plus water; for the HREELS work, 0.01 M H_2SO_4 was employed. Chemisorption was carried out at open circuit for 180 seconds. Prior to HREELS experiments, unadsorbed material was removed by copious rinses with ultrapure water.

Electrochemical control was accomplished by a BAS CV-27 (Bioanalytical Systems, West Lafayette, IN). Potentials were referenced to a Ag/AgCl (1.0 M NaCl) electrode in a compartment separated from the working electrode by a fine glass frit to inhibit Cl^- contamination. A Pt wire was employed as an auxiliary electrode.

Computational method

In contrast to *ab initio* methods, density functional theory simplifies the solution of the time-independent Schrödinger equation by an approximation of the ground-state electron density (ρ) in the Hohenberg–Kohn formulation of the wavefunction, molecular energy, and other ground-state properties of the system.[20] In DFT, the external potential of a system can be obtained directly from ρ; hence, all properties of the system derived from the Schrödinger equation can be determined using ρ. The ground-state total energy (E_t) of the system can thus be calculated based on the electron density:

$$E_t[\rho] = T[\rho] + U[\rho] + E_{XC}[\rho] \quad (1)$$

where $T[\rho]$ is the kinetic energy, $U[\rho]$ the electrostatic energy, and $E_{XC}[\rho]$ the exchange and correlation energy arising from non-interacting particles, Coulombic interactions, and many-body contributions.[20,21] The Kohn–Sham equations represent single-particle wavefunctions that can be solved self-consistently to calculate the energies.[22]

$T[\rho]$ and $U[\rho]$ of a given system can easily be established but not $E_{XC}[\rho]$. This means that $E_t[\rho]$ can be calculated (minimized) only after an appropriate approximation for $E_{XC}[\rho]$ is obtained. In this work, the Cambridge Sequential Total Energy Package (CASTEP), a first-principles DFT code integrated in Material Studio 5.0 (Accelrys Inc., San Diego, CA), was employed to perform the calculations;[23] the generalized gradient approximation (GGA)[24] and the Perdew–Wang exchange–correlation functional, PW91,[25] were used to approximate $E_{XC}[\rho]$. The plane-wave basis set was adopted to represent the wavefunctions, and Vanderbilt-type pseudopotentials were employed to describe the external potential of the periodic system as well as allow computations at lower cutoff energies.

Minimization of the total energy with respect to changes in geometry is the crux of this approach: the lowest-energy state is the most probable structure. In the calculations, geometry

optimization was performed with a cutoff energy of 450 eV and with the Broyden–Fletcher–Goldfarb–Shanno (BFGS) method as the energy minimization algorithm. The Monkhorst–Pack grid and Fermi smearing were set to (3 × 3 × 1) and 0.1 eV, respectively. As a standard for convergence, the tolerance in energy, force, and displacement were 1.0×10^{-5} eV atom^{-1}, 0.03 eV Å^{-1}, and 0.001 Å, respectively. All parameters were sufficient to attain a reasonable convergence in the determination of the optimized structure and the total energy.[13,26–28]

A (3 × 3) supercell was used in the calculations to model the adlattice structures on the Pd(111) surface. A metal slab consisting of four layers of Pd atoms, where only the upper two Pd layers were allowed to relax, represented the Pd(111) surface. A vertical vacuum space of *ca.* 15 Å separated the metal slab from its periodic images[13,26–28] and the adsorbed molecules were placed in this vacuum space. A slab model was used since it overcomes many of the difficulties faced in cluster models.[29,30]

The adsorption energy (E_{ads}) determines the relative stabilities of the adsorption structures and is defined as:

$$E_{ads} = E_{M-A} - E_A - E_M \quad (2)$$

where E_{M-A}, E_A and E_M, respectively, correspond to the total energies of the surface organometallic compound, the unadsorbed species, and the clean (111) metal surface. The most favorable structure is identified by the lowest E_{ads}.

Vibrational frequencies were calculated from the (Hessian) matrix of Cartesian second derivatives of a periodic or molecular system;[31,32] in this study, the finite-displacement method[32] was employed to calculate the vibrational frequencies and vibrational states in the interfacial system.

Results and discussion

The Γ *vs.* log($C°$) chemisorption isotherm of 2,3-dimethylhydroquinone on a Pd(pc) electrode is shown in Fig. 2. It is obvious that the isotherm is characterized by two constant-Γ plateaus: At concentrations below 0.05 mM, $\Gamma_{plateau}$ is approximately 0.18 nmol cm^{-2} ($\sigma_{plateau}$ = 92.2 Å^2); above 0.5 mM, $\Gamma_{plateau}$ is *ca.* 0.51 nmol cm^{-2} ($\sigma_{plateau}$ = 32.5 Å^2). These values, respectively, indicate flat-configured adsorbates at low concentrations ($\sigma_{flat,calc}$ = 68.7 Å^2) and 5,6-edge-vertical orientations at high concentrations ($\sigma_{edge,calc}$ = 33.6 Å^2). Since there is no actual 2,3-dimethylhydroquinone orientation that would yield a molecular cross section larger than $\sigma_{flat,calc}$, the significantly higher experimental value of 92.2 Å^2 can only mean that the organic monolayer is constituted by loosely packed parallel-oriented molecules. Evidently, there are substantial adsorbate–adsorbate repulsive interactions, most likely because of the motionally restricted methyl groups, and that the strength of the metal–organic bond in the flat orientation is not sufficient to the overcome such repulsions at full, close-packed, coverage. The repulsive interactions are minimal in the edge orientation probably because phenyl–methyl single bond is rotationally unrestricted.

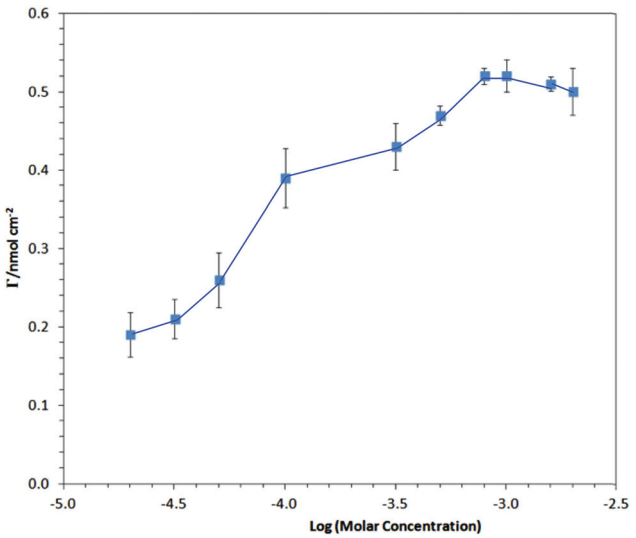

Fig. 2 Chemisorption isotherm, Γ *vs.* log $C°$ plot, for 2,3-dimethylhydroquinone at a smooth polycrystalline Pd electrode. TLE volume: 3.56 µL. Electrode surface area: 1.26 cm^2. The solid lines merely interconnect the data points and do not imply any theoretical fit.

HREELS spectra of a Pd(111) electrode surface emersed from 0.05 mM, 0.5 mM and 5 mM solutions of the subject compound are displayed in Fig. 3. The notable peaks that are common to all three spectra are at 2969, 1429, 1223, and 611 cm^{-1}. The first three correspond to methyl-group vibrations, respectively, C–H stretch, C–C stretch, and C–H bend; the peak at 611 cm^{-1} represents the aromatic out-of-plane C–H bend, γ(CH). For the present study, only γ(CH), was selected for the surface coverage determinations because the other modes are associated with the methyl groups, and are essentially insensitive to orientation effects. The areas under the peaks were obtained by valley-to-valley baseline integration *via* Origin software (OriginLab, Northampton, MA, USA). The normalized areas (A_N) can be converted to surface concentrations (Γ) by the relationship $\Gamma_{HREELS} = kA_N$, where k is a cali-

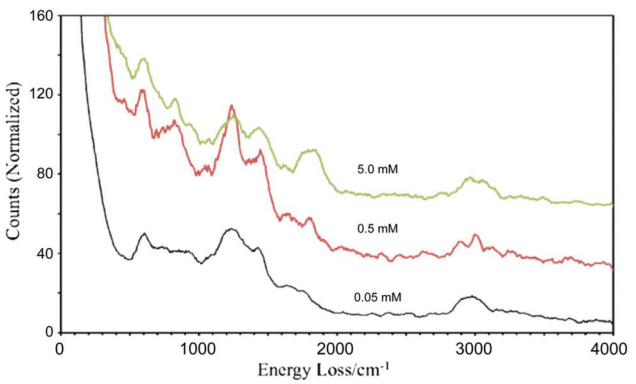

Fig. 3 HREELS spectra of Pd(111) surfaces emersed from 0.05 mM, 0.5 mM, and 5.0 mM aqueous solutions of 2,3-dimethylhydroquinone. Experimental conditions: primary beam energy = 4 eV, primary beam current = 100 pA, specular geometry = 62° from surface normal, resolution = 4.8 meV (38 cm^{-1}).

bration factor.[12] To compare Γ_{TLE} with Γ_{HREELS}, the proportionality constant need not be determined if Γ_{TLE} and Γ_{HREELS} are expressed in their normalized forms, $\Gamma_{TLE}/\Gamma_{TLE,Lowest}$ and $\Gamma_{HREELS}/\Gamma_{HREELS,Lowest}$, where the denominators are the lowest values measured. Since $\Gamma_{HREELS}/\Gamma_{HREELS,Lowest} = A_N/A_{N,Lowest}$, comparison can just be made between $\Gamma_{TLE}/\Gamma_{TLE,Lowest}$ and $A_N/A_{N,Lowest}$ for any given point in the chemisorption isotherm. The good agreement between the TLE and HREELS results in terms of morphology and numerical values was as expected from a previous study.[12]

It may be noted that, while an edge-attached diphenol supposedly exists on the surface at higher coverages, there is no evidence in the HREELS spectra for the presence of the –OH group. The reason for this is unclear. It should just be pointed out that, for 2-mercapto-1,4-diphenol which, on Pd, is attached through the –SH group with the diphenol moiety intact and pendant, as evidenced by its reversible quinone/diphenol redox reaction, no HREELS-active –OH stretch was seen at potentials where only the diphenol existed; but, at potentials where only the quinone would be present, a prominent C=O peak was observed.[5] In other words, the absence of an –OH peak for edge-adsorbed 2,3-dimethylhydroquinone does not necessarily indicate a quinone since a C=O peak was not observed either. This issue needs to be investigated further by other surface spectroscopic methods.

Several possible adsorption sites and structures of 2,3-dimethyl-1,4-benzoquinone (Fig. 4) were modeled and geometrically optimized by DFT. Holl, Bri, and Atop represent structures in which the quinone ring is centered on three-fold hollow, two-fold bridge, and atop sites, respectively; 0 and 30 correspond to the angle of the compound's peripheral C–H, C=O, or C–CH_3 bonds relative to the [110] direction of the metal substrate. In some structures, there are two possible locations for the carbonyl oxygen; these are labeled A and B to differentiate the two geometries. The calculated adsorption energies of the structures in Fig. 3 are presented in Table 1.

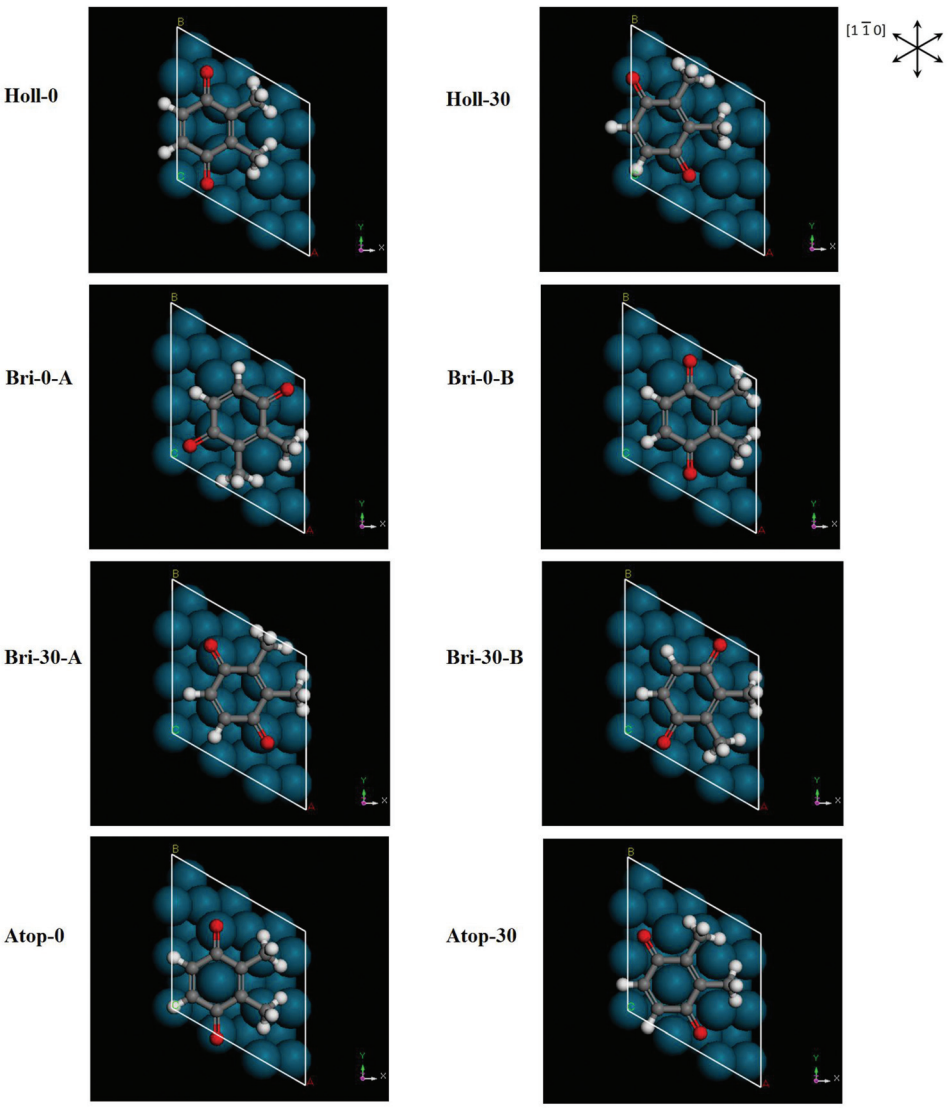

Fig. 4 Possible adsorption structures of flat-oriented 2,3-dimethyl-1,4-benzoquinone on Pd(111).

Table 1 DFT-calculated adsorption energy (eV) of 2,3-dimethyl-1,4-benzoquinone at various adsorption sites on Pd(111)[a]

Adsorption structure	Adsorption energy (E_{ads})
Holl-0	−0.28
Holl-30	No stable structure
Bri-0-A	−0.11
Bri-0-B	No stable structure
Bri-30-A	−0.38
Bri-30-B	−0.70
Atop-0	No stable structure
Atop-30	No stable structure

[a] All calculations were performed using a 3 × 3 surface unit cell with a fixed cell volume equal to that of a bare Pd surface. The energy of the 2,3-dimethyl-1,4-benzoquinone molecule was calculated separately in a 12 × 12 × 12 Å^3 cell.

Bri-30-B was found to have the most negative adsorption energy (−0.70 eV) and is thus considered as the most favorable surface organometallic structure.

Fig. 5 shows the optimized structure of 2,3-dimethyl-1,4-benzoquinone chemisorbed parallel to the surface. Close inspection reveals that, similar to those found for benzene, *p*-benzoquinone, and *p*-benzoquinone sulfonate, the peripheral bonds of the quinone ring are bent away from the surface, but the ring itself is not tilted;[13,26,28] the aromatic molecule remains bonded to the surface through the two double bonds of the quinone. Perhaps due to the presence the comparatively bulkier methyl groups, C–CH_3 bonds are bent farther from the surface than the C–H bonds.

Fig. 6 shows the optimized structure of (5,6-η)-*o*-phenylene organopalladium, the DFT-generated model for the edge-oriented diphenol. It is the sole energetically stable structure at this orientation, and the molecule is centered on a bridge site. It is important to emphasize that only the C–H bonds in the ring are activated and metalated, since such processes *via* the methyl C–H bonds yield highly unstable surface structures. This also helps explain why tetramethyl-1,4-dihydroxybenzene does not yield edge-adsorbed surface organometallic compounds.[1]

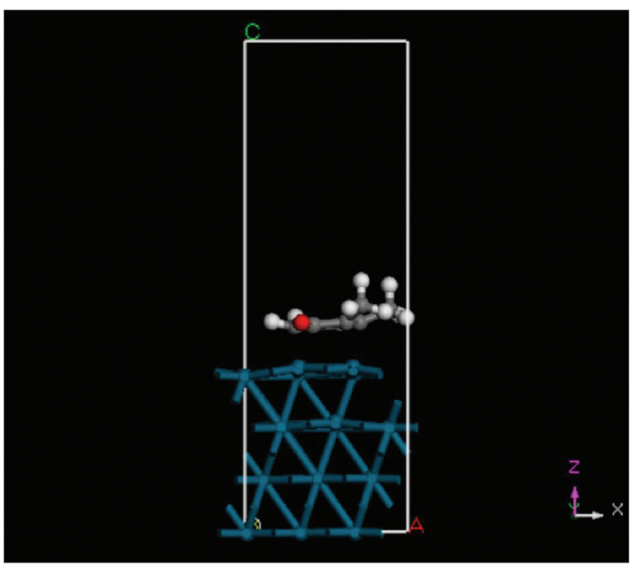

Fig. 5 Optimized adsorption structure of the flat-adsorbed 2,3-dimethyl-1,4-benzoquinone (Bri-30-B) on the Pd(111) surface.

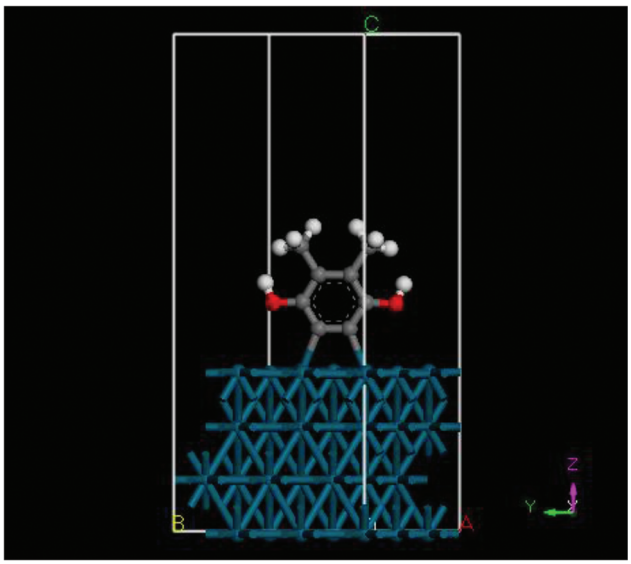

Fig. 6 Optimized adsorption structure of the 5,6-edge-oriented 2,3-dimethylhydroquinone molecule on the Pd(111) surface.

The calculated vibrational spectra for the flat-adsorbed quinone and edge-oriented diphenol are shown in Fig. 7 and 8, respectively. The most notable difference between the two is that the highest vibrational frequency associated with a carbon–carbon bond is 1458 cm^{-1} for the flat-adsorbed quinone, but it is almost 200 cm^{-1} higher for the edge-oriented diphenol. The former represents a dipole-active $C_{Quinone}$–C_{Methyl} stretch vibration while the latter typifies an aromatic-ring breathing (in-plane C=C stretch) mode. Experimental validation is afforded by the HREELS spectra in Fig. 3 which indicate that the area under the peak at *ca.* 1700 cm^{-1} is much higher for chemisorption at 5 mM than at 0.5 mM, and that it is non-existent at 0.05 mM. This behavior is rationalized by the metal-surface dipole selection rule which states that only vibrations normal to the surface are HREELS-active:[32] The quinone-ring breathing mode is parallel to the surface for the flat-adsorbed molecule and is HREELS-inactive; it becomes HREELS-active in the vertical diphenol orientation since the aromatic-ring breathing mode is now perpendicular to the surface.

Summary

The chemisorption of 2,3-dimethyl-1,4-dihydroxybenzene from aqueous sulfuric acid solution onto Pd(pc) and Pd(111) electrode surfaces has been investigated by thin-layer electrochemistry, high-resolution electron energy loss spectroscopy,

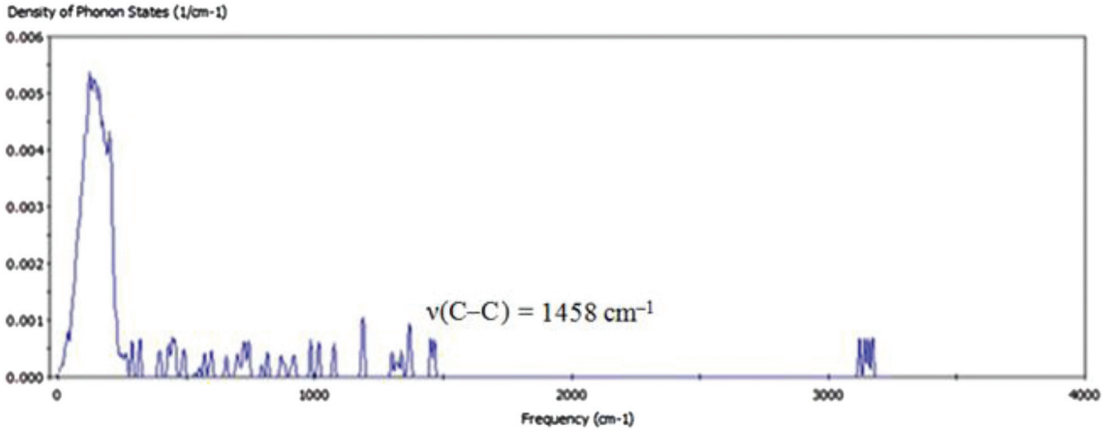

Fig. 7 Computed vibrational spectrum of the flat-adsorbed 2,3-dimethyl-1,4-benzoquinone on Pd(111).

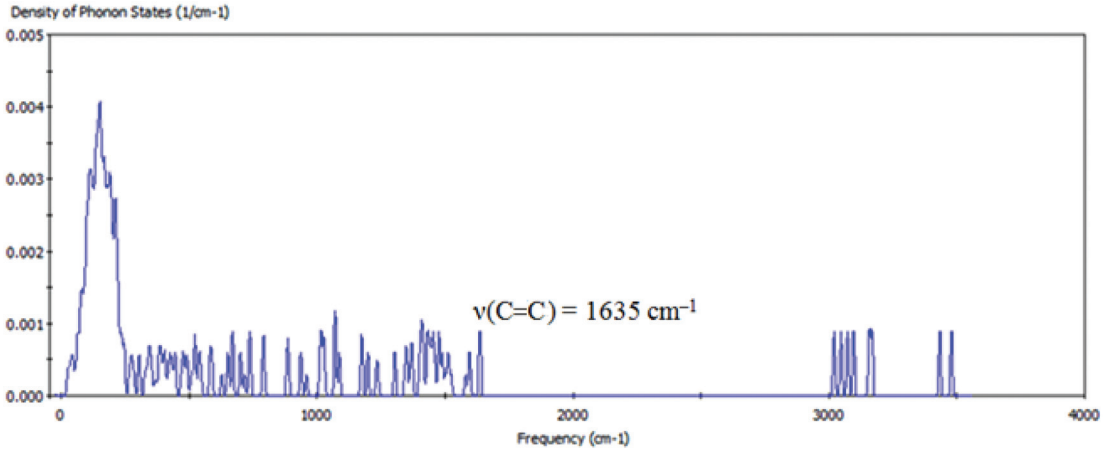

Fig. 8 Computed vibrational spectrum of the 5,6-edge-attached 2,3-dimethylhydroquinone on Pd(111).

and density functional theory. When chemisorption was from low concentrations, the diphenol was oxidatively adsorbed as the quinone in the flat orientation, analogous to a (2,3,5,6-η)-2,3-dimethyl-*p*-quinone palladium complex. At elevated concentrations, chemisorption was also oxidative but in the edge-vertical orientation, similar to a (5,6-η)-*o*-phenylene organopalladium compound in which the C–H bonds at the 5 and 6 ring positions are activated and palladium-surface-metalated.

Acknowledgments

This material is based upon work performed by the Joint Center for Artificial Photosynthesis, a DOE Energy Innovation Hub, as follows: The surface organometallic work, spectroscopic interpretations and DFT analysis were supported through the Office of Science of the U.S. Department of Energy under Award No. DE-SC0004993; the TLE and HREELS experiments were supported by the Texas A&M University-CONACYT program (MPS).

References

1 M. P. Soriaga, E. Binamira-Soriaga, A. T. Hubbard, J. B. Benziger and K. W. P. Pang, *Inorg. Chem.*, 1985, **24**, 65.
2 M. P. Soriaga, J. H. White, V. K. F. Chia, D. Song, P. O. Arrhenius and A. T. Hubbard, *Inorg. Chem.*, 1985, **24**, 73.
3 J. F. Rodriguez, J. E. Harris, M. E. Bothwell, T. Mebrahtu and M. P. Soriaga, *Inorg. Chim. Acta*, 1988, **148**, 123.
4 M. P. Soriaga, *Chem. Rev.*, 1990, **90**, 771.
5 J. E. Soto, D. Li, J. Sanabria-Chinchilla, X. Chen and M. P. Soriaga, *J. Mol. Struct.*, 2008, **890**, 298.
6 M. P. Soriaga and A. T. Hubbard, *J. Am. Chem. Soc.*, 1982, **104**, 3937.
7 M. P. Soriaga and A. T. Hubbard, *J. Am. Chem. Soc.*, 1982, **104**, 2735.
8 M. P. Soriaga and A. T. Hubbard, *J. Phys. Chem.*, 1984, **88**, 1089.
9 M. P. Soriaga, J. H. White, D. Song and A. T. Hubbard, *J. Phys. Chem.*, 1984, **88**, 2284.
10 M. P. Soriaga, J. H. White, D. Song and A. T. Hubbard, *J. Phys. Chem.*, 1984, **88**, 2284.

11 K.-W. P. Pang, J. B. Benziger, M. P. Soriaga and A. T. Hubbard, *J. Phys. Chem.*, 1984, **88**, 4583.
12 J. Sanabria-Chinchilla, X. Chen, D. Li and M. P. Soriaga, *Electrocatalysis*, 2013, **4**, 101.
13 A. Javier, Y.-G. Kim, J. H. Baricuatro, P. B. Balbuena and M. P. Soriaga, *Electrocatalysis*, 2012, **3**, 353.
14 M. P. Soriaga, V. K. F. Chia, J. L. Stickney, S. D. Rosasco, G. N. Salaita, A. T. Hubbard, J. B. Benziger and K. W. P. Pang, *J. Electroanal. Chem.*, 1984, **163**, 407.
15 J. Sanabria-Chinchilla, Y. G. Kim, X. Chen, H. Baltruschat and M. P. Soriaga, *Mod. Asp. Electrochem.*, 2010, **48**, 8.
16 A. Javier, D. Li, P. B. Balbuena and M. P. Soriaga, *Electrocatalysis*, 2010, **1**, 159.
17 A. T. Hubbard, *Crit. Rev. Anal. Chem.*, 1973, **3**, 201.
18 M. P. Soriaga and R. J. Barriga, in *Handbook of Surface Imaging and Visualization*, ed. A. T. Hubbard, CRC Press, Boca Raton, FL, 1995, ch. 34.
19 J. Jungwirthova and L. L. Kesmodel, *J. Phys. Chem. B*, 2001, **105**, 674.
20 P. Hohenberg and W. Kohn, *Phys. Rev. B*, 1964, **136**, 864.
21 W. Kohn and L. J. Sham, *Phys. Rev. A*, 1965, **140**, 1133.
22 M. Levy, *Proc. Natl. Acad. Sci. U. S. A.*, 1979, **76**, 6062.
23 S. J. Clark, M. D. Segall, C. J. Pickard, P. J. Hasnip, M. J. Probert, K. Refson and M. C. Payne, *Z. Kristallogr.*, 2005, **220**, 567.
24 J. P. Perdew, K. Burke and M. Ernzehof, *Phys. Rev. Lett.*, 1996, **77**, 3865.
25 J. P. Perdew and Y. Wang, *Phys. Rev. B: Condens. Matter*, 1992, **45**, 13244.
26 A. Javier, D. Li, P. B. Balbuena and M. P. Soriaga, *Electrocatalysis*, 2010, **1**, 159.
27 H. Q. Qian, H. Y. Mao, F. Song, S. Q. Shi, H. J. Zhang, H. Y. Li, P. M. He and S. N. Bao, *Appl. Surf. Sci.*, 2010, **256**, 2686.
28 C. Morin, D. Simon and P. Sautet, *J. Phys. Chem. B*, 2003, **107**, 2995.
29 R. A. Evarestov, Th. Bredow and K. Jug, *Phys. Solid State*, 2001, **43**, 1774.
30 J. Z. Sexton and A. C. Kummel, *J. Vac. Sci. Technol., B*, 2003, **21**, 1908.
31 E. B. Wilson, J. C. Decius and P. C. Cross, *Molecular Vibrations*, Dover, New York, 1955.
32 H. Ibach and D. L. Mills, *Electron Energy Loss Spectroscopy and Surface Vibrations*, Academic Press, New York, 1982.